

FEM explicit dynamic simulation of micro shot peening: a stochastic approach

M. Marini ^a, V. Fontanari ^a, M. Bandini ^b, M. Benedetti ^a

^a University of Trento, Italy, m.marini@unitn.it, matteo.benedetti@unitn.it, vigilio.fontanari@unitn.it;

^b Peen Service s.r.l., Italy, m.bandini@peenservice.it

Keywords: Shot peening, Finite element method (FEM), explicit dynamic, surface roughness, residual stress

Introduction

At the beginning of the research on the FEM simulation of the shot peening process, the *symmetry cell* approach, devised in the studies of Meguid [1], was used by many authors to estimate the residual stress (RS) field. The study of Bagherifard [2] underlined the need for a realistic FE model, based on statistical considerations, which was used in the following studies by many authors, such as Bagherifard [3], Garipey [4], Peñuelas [5].

Numerical investigations undertaken so far have mainly addressed surface treatments using steel shots with a diameter larger than 0.5 mm. On the other hand, several experimental investigations have pointed out that light alloys benefit more from gentle peening treatments employing small ceramic beads with a diameter lower than 0.15 mm, often referred to as micro- or fine-particle shot peening. Indeed, such treatments introduce a compressive RS peak located close to the surface where the cracks are likely to nucleate and induce a less detrimental surface roughening. Clearly, the numerical analysis of micro shot peening represents a tremendous computational challenge given the large number of impacts to be simulated to achieve complete coverage and the very fine mesh required for the FE model to appreciate low surface roughness and thin surface layers affected by the compressive RS. The outcomes of FE models are usually validated by comparison with in-depth RS measurements undertaken with diffractometric techniques, but often the effect of radiation penetration into the sample is overlooked. This can lead to significant errors if the numerically estimated RSs are directly compared with measures taken on light alloys characterized by X-Ray penetration depth (on the order of tens of microns) comparable with the thickness of the surface layer where the compressive RS develops. On the other hand, the simulation of micro-shot peening treatments would be of great industrial interest, as the effects of the fundamental process parameters could be estimated without requiring expensive experimental techniques. In addition, the numerical reproduction of the surface morphology would allow a direct estimation of the stress concentration effect at surface dimples in place of semi-analytical simplified models based on large-scale roughness parameters, whose applicability to micro-shot peening treatments has yet to be validated.

Objectives

The present paper is aimed at developing a FEM procedure to simulate a micro-shot peening process, introducing in the simulation also the stochastic aspects of the treatment, in order to obtain a realistic and significant numerical analysis. The peening process, termed CE-B120, is applied to the aeronautical grade Al-7075-T651 aluminium alloy. This treatment has proved to be very effective in improving the fatigue resistance of Al-alloys with respect to conventional steel shots, as the use of ceramic beads, prevents dangerous galvanic effects, and small peening media confer a shallow and intense compressive RS peak without excessive surface roughening [6]. The results of the dynamic simulations were processed to estimate the plastic layer thickness, the surface roughness and the RS state. To consistently compare experimental and numerical estimations of the RS field, the effect of radiation penetration and surface roughness was considered according to an approach specifically devised in this paper.

Methodology

As regards the experimental part of the study, shot peening is applied to Al-7075-T651 hourglass prismatic specimens. Monotonic tensile and mass properties of the target material are tested as well as the cyclic stress-strain behaviour of the material, as reported in [7]. Shot peening is carried out using fused ceramic micro-beads B120, having composition 67% ZrO_2 31% SiO_2 , Young's modulus 300 GPa and hardness 700 HV. The size distribution of the beads is estimated through a granulometric analysis using a Rotap sieve shaker. Measures are carried out according to the standard ASTM-C-136 using 6 sieves with decreasing size comprised between 150 and 53 μm . The beads are propelled with a mass flow rate of 5 kg/min onto the target surface by an air-blast machine equipped with a Tetra nozzle with 12 mm diameter and operating at 100 mm working distance. Shot velocity is measured by means of a DSLR camera based equipment. Surface roughness of the peened surface is characterized through 2D and 3D measurements, using a contact profilometer and a confocal optical [8]. The in-depth RS profile induced by the shot peening treatment is measured through an X-ray diffraction analysis, as reported in [9]. The thickness of the layer where the RSs develop is comparable with the penetration depth of the radiation into Al, viz. about 12 μm . To make possible a direct comparison with the residual stresses estimated by the numerical analyses, the deconvolution techniques proposed in [6] is adopted to estimate the true in-depth residual stress profile.

The dynamic FE simulations are carried out with the explicit Ansys/LS-Dyna® 17 commercial software. The FE model consists in a target body, representing a part of the peened component, and in a certain number of beads impinging on it, as shown in Fig. 1. The target is modelled as a square-based prism, with 300 μm side and 240 μm height. The impacts are confined in a circular area of 110 μm diameter in the center of the target upper face, hereinafter denoted as impact area. All the bodies are meshed with 4 nodes brick elements SOLID164 with reduced integration and hourglassing control. The prismatic volume encompassing the impact area, with 156 μm side and 120 μm height, is finely meshed with 1.3 μm size elements, while the surrounding volume of the target body is discretized with elongated elements. The fine-mesh element size is about 1/20 of the average impact dimple diameter as suggested in [3] to have a good resolution of the RS state. The boundary of the target volume is constrained to prevent normal nodal displacements in order to take into account the constraint exerted by the surrounding material, and silent boundaries are applied on all the constrained surfaces to prevent the reflection of the shock waves. A surface-to-surface automatic contact couple is established between the target surface and each bead surface, where the beads represent the master surface.

An artificial elastic-plastic behaviour is implemented for the ceramic shots, in order to increase the solver stability, as suggested by some empirical experience. A bilinear elastoplastic model is assumed, with very high yield strength (3 GPa) and tangent modulus (30 GPa), chosen to make the plastic deformation negligible. Particular care is taken in modelling the elastic-plastic behavior of the target material. Since experiments did not reveal pronounced anisotropy and strain rate sensitivity of the Al-7075 alloy, these last two effects are neglected. Many authors adopted the Johnson-Cook or the Cowper-Symonds model to take into account strain rate sensitivity. However, both models rely on a purely isotropic hardening law, while peened parts are subject to repeated impacts, experiencing complex non-monotonic load histories. Under these conditions, the strain-hardening of most metallic materials displays a significant kinematic component effect. Comparing the experimental stress-strain curves with the ones obtained from the FE model applying the Johnson-Cook model, the excessive material hardening is evident Fig. 2A. In view of these observation, we decided to adopt the Lemaitre-Chaboche mixed hardening model [10] to incorporate both kinematic and isotropic hardening components. The model parameters are obtained through a trial and error tuning procedure using a FE model simulating the strain-controlled axial test. The very good agreement of the numerical model with the experimental data is shown in Fig. 2B.

A MatLab routine is developed to create, prior to the FEM simulation, sets of shots capable to achieve the 100% nominal coverage on the circular area of 100 μm of radius, in the center of the upper surface

of the target body, denoted as the control area. Each set is a bunch of data, containing the impact point coordinates, the dimension and velocity of the shots. The script at first randomly assigns the dimension value to the first bead on the base of the stochastic size distribution. A Weibull cumulative distribution function is fitted to the shot size distribution: shot dimensions in the model are chosen between 53 and 125 μm , in order to avoid the generation of unrealistically large or ineffective small beads. The shot velocity is assumed to be normally distributed, with mean 57 m/s and standard deviation $\sigma=2.5\text{m/s}$. The velocity values are chopped below 52 m/s and above 62 m/s, in conformity with experimental observations. A specific simulation campaign is carried out to estimate the dimple dimension on the base of the shot dynamics. Using three levels for both shot size and velocity, 9 single impact 2D axisymmetric simulations are carried out. Through a linear regression, it is possible to compute the coefficients of the bilinear function that links the dimple diameter to the shot radius and velocity. This function is used by the MatLab routine to compute the dimension of the dimple caused by the impact of shots randomly located inside the control area. The shots are stacked up over the target, equally spaced out along the height direction. From the speed and the distance from the surface, it is possible to evaluate quite precisely the impact time of each shot. Previous studies [1] showed that it is not indispensable to consider the interaction among shots, as long as the shots do not interfere in the impact stage [3]. Therefore, the shots interpenetrate when stacked, and no interaction is considered among them; however, a check is performed to prevent two or more shots from imping at the same time in the same place. The number of shots generated in each simulation is the minimum number to achieve full coverage. It is worth noting that the applied method does not consider at all the effect of material strain hardening, even if it is not rare to observe overlapping dimples (both in the simulation and in the experimental practice). However, only the not-overlapping part of every dimple really affects the coverage evaluation, being the overlapping part already considered in the previous impingement. Moreover, the strain hardening in the alloy is not very marked, and is supposed not to affect significantly the dimension of the dimples. When the MatLab routine reaches the desired coverage level, the FEM simulation is started.

Only the mass matrix damping is used, and it is empirically tuned to obtain an effective damping ratio having a subcritical oscillation regime. The final value is set to $\alpha=24 \cdot 10^6 \text{ s}^{-1}$.

Very little information is available about the tribological conditions. A set of 4 simulation is processed with 6 different values of friction. By comparison of these simulation results (RSs and roughness) to the experimental data, a value of 0.05 is chosen for the friction coefficient.

30 randomly generated explicit dynamic simulations are carried out to achieve statistical significance for all the stochastic phenomena involved.

After the dynamic simulations, an implicit procedure is performed to compute the stress concentration factor K_t . The finely meshed volume of the target body is exported into the static implicit simulation environment. The new model has roughly the shape of a square based parallelepiped, and preserves the deformed shape of the previous model but not the residual stress state. The model undergoes two static simulations, consisting in the application of a uniform tensile stress of 1 MPa on two opposite side faces, first in the x then in the z direction. The simplest method for the estimation of the K_t factor consists in computing the ratio between the nominal stress applied to the model and the maximum equivalent stress in the model. This method leads to a large overestimation of the stress concentration factor, since it considers the stress state that develops in very small volumes. For a better estimate of the K_t , as proposed in [11], the theory of critical distance is applied, in which the stress averaging domain is a circular area lying on the plane normal to the direction of load application and centred in the crack initiation site. The size of this circular area was estimated equal to 54 μm for the high-cycle fatigue strength of Al-7075-T651. The equivalent von Mises stress is averaged over the half-circular area centred in the bottom of the crater characterized by the highest stress value and therefore in the most likely crack initiation site Fig. 3A.

Results and analysis

The nodal results are extracted from the control volume under the control area.

The 2D and 3D roughness parameters are evaluated considering out-of-plane displacements of nodes lying on two orthogonal diameters and on the whole control area, respectively.

Roughness parameter	FEM average value (μm)	FEM standard deviation (μm)	FEM Max value (μm)	Experimental value (μm)	Experimental standard deviation (μm)	Error %
R_a	0.98	0.22	1.48	1.35	0.14	-27.4
S_a	1.02	0.11	1.29	1.24	0.05	-17.7

The simulation slightly underestimates the actual surface roughness. However, the experimental values are well estimated by the maximum recorded surface roughness obtained in the simulations, and they also lie inside the 96% confidence interval. The systematic underestimation of the surface roughness can be, at least partly, imputed to the FEM discretization of the target surface. Even if the impact area is finely meshed, the size of the elements may not be able to entirely capture the sharp peaks of the impinged surface.

The in-depth RS profile, in some papers, is evaluated considering the undeformed configuration of the target. This issue is marginal in conventional shot peening, but in micro shot peening treatments, the depth of the surface layer, where significant nodal displacement take place, is comparable to that interested by compressive RSs; therefore, a realistic estimation of the RS profile requires the nodal displacements to be considered. In addition, the effect of X-ray penetration on the RS measurements must be considered for a consistent comparison of experimental and numerical data. Three strategies are applied to address these issues. The first one consists in ideally “slicing” the control volume in 2 μm thick layers starting from the highest peak on the surface and proceeding towards the specimen depth. Averaging the nodal stress value in every slice, the RS profile is obtained as a function of the depth below the surface. This profile is compared with the profile obtained in [6]. Fig. 4A shows experimental data corrected for penetration of the X-rays and the numerical estimates corrected for layer deformation. The 95% confidence interval of the numerical profile is almost completely comprised in that of the experimental measure. The depth of surface layers interested by compressive RSs (about 50 μm) and the intensity of compressive RS peak (about -400 MPa) are well reproduced by the numerical simulations, while these underestimate the peak location below the surface (12 vs 20 μm) and overestimate the compressive RSs in the outer 10 μm thick layer.

The second strategy consists in considering the X-ray penetration by processing the nodal stresses to obtain a RS profile comparable with the experimental profile raw from the XRD measurements. At each depth below the surface, the RS value is computed by numerical integration of the convolution integral reported in [6], whereby the integral is replaced by the following weighted average of discrete RS estimations:

$$\bar{\sigma}_{xx}(z) = \frac{\sum_{i=1}^N \sigma_i e^{-\frac{z-z_i}{\xi}}}{\sum_{i=1}^N e^{-\frac{z-z_i}{\xi}}} \quad (1)$$

where N is the number of nodes laying deeper than the chosen y value, y_i and σ_i are respectively the depth and the RS value for each of the selected nodes and ξ is the information depth discussed in [6]. Fig. 4B compares raw experimental RS data with the numerical estimations done according to this second strategy, namely corrected for layer deformation and X-ray penetration. Also in this case, the agreement is very good, especially in terms of overlapping between the confidence intervals, apart from a very superficial layer (8 μm thickness), where the simulations overestimate the compressive RSs. This could be related to the fact that the structure of this layer is greatly affected by the surface roughness, as its thickness is comparable with the maximum peak-to-valley distance.

The last approach attempts to consider the effect of both surface roughness and radiation penetration on the XRD measurement of the RS profile. Specifically, the outer surface layers are not continuous owing to the irregular surface morphology composed of peaks and valleys. Surface layers can then be

referred to as a continuum of pseudo-density lower than that of the bulk. For this reason, they are expected to contribute less to the RS information collected by the XRD technique. Therefore, in a first approximate attempt to estimate the true RS profile, the contribution of each material layer to the XRD measure is scaled proportionally to its pseudo-density. To evaluate this parameter, the control volume is divided into thin slices (1 μm) and the material continuity is estimated as the ratio of the number of nodes in every slice to the number of nodes on the undeformed surface. The stress value of each material layers is scaled as follows:

- 1) the penetration coefficient ξ is supposed to be related to the actual material density, being the material a filter to the radiation penetration, so for each material layer a different ξ_l coefficient is:

$$\xi_l = \frac{N_{surf}}{N_l} \quad (2)$$

where ξ_l is the penetration coefficient for the l -th layer, N_l is the number of nodes in the l -th layer and N_{surf} is the number of nodes on the undeformed surface;

- 2) The RS is thus computed from the following expression:

$$\sigma_{xx}(z) = \frac{N_{pv}}{N_u} \frac{\sum_{i=1}^N \sigma_i e^{-\frac{z-z'}{\xi_i}}}{\sum_{i=1}^N e^{-\frac{z-z'}{\xi_i}}} \quad (3)$$

where N_{pv} is the number of nodes having height lower than the highest peak and higher than the deepest valley, and N_u is the number of nodes enclosed in the same volume when undeformed.

This last method is adopted in the comparison shown in Fig. 4C. The stress profile seems somehow artificial, indicating the need of a more sophisticated algorithm in the pseudo-density computation. Anyway, the stress profile correction moves in the right direction, reducing the surface stress value. Finally, the plot representing the K_t parameter versus the radius of the hemi-circular area is shown in Fig. 3B. The results obtained from the FEM (Fig.3B(b)), which gives a K_t value of 1.05 for a 54 μm radius, show good accordance with the experimental/empirical results. The semi-analytical approach devised in [6] predicts a value of 1.11 (Fig. 3B(c)) with similar roughness parameters, while the 2D FEM model developed in [11] using the experimental surface profiles estimates a K_t value of 1.09 (Fig. 3B(d)). The slight discrepancy of FE predictions from experimental measures is related to the underestimation of the surface roughness, which is supposed to influence the stress concentration.

References

- [1] S. A. Meguid, G. Shagal, and J. C. Stranart, "3D FE analysis of peening of strain-rate sensitive materials using multiple impingement model," *Int. J. Impact Eng.*, vol. 27, no. 2, pp. 119–134, 2002.
- [2] S. Bagherifard, R. Ghelichi, and M. Guagliano, "On the shot peening surface coverage and its assessment by means of finite element simulation: A critical review and some original developments," *Appl. Surf. Sci.*, vol. 259, pp. 186–194, 2012.
- [3] S. Bagherifard, R. Ghelichi, and M. Guagliano, "A numerical model of severe shot peening (SSP) to predict the generation of a nanostructured surface layer of material," *Surf. Coatings Technol.*, vol. 204, no. 24, pp. 4081–4090, 2010.
- [4] A. Gariépy, S. Larose, C. Perron, and M. Lévesque, "Shot peening and peen forming finite element modelling - Towards a quantitative method," *Int. J. Solids Struct.*, vol. 48, pp. 2859–2877, 2011.
- [5] I. Peñuelas, P. Sanjurjo, C. Rodríguez, T. E. García, and F. J. Belzunce, "Influence of the target material constitutive model on the numerical simulation of a shot peening process," *Surf. Coatings Technol.*, vol. 258, pp. 822–831, 2014.
- [6] M. Benedetti, V. Fontanari, B. Winiarski, M. Allahkarami, and J. C. Hanan, "Residual stresses reconstruction in shot peened specimens containing sharp and blunt notches by experimental measurements and finite element analysis," *Int. J. Fatigue*, vol. 87, pp. 102–111, 2016.
- [7] M. Benedetti, V. Fontanari, and B. D. Monelli, "Numerical Simulation of Residual Stress Relaxation in Shot Peened High-Strength Aluminum Alloys Under Reverse Bending Fatigue," *J. Eng. Mater. Technol.*, vol. 132, no. 1, pp. 11012-1–9, 2010.

- [8] M. Benedetti, V. Fontanari, M. Bandini, and D. Taylor, "Multiaxial fatigue resistance of shot peened high-strength aluminum alloys," *Int. J. Fatigue*, vol. 61, pp. 271–282, 2014.
- [9] M. Benedetti, V. Fontanari, M. Bandini, and E. Savio, "High- and very high-cycle plain fatigue resistance of shot peened high-strength aluminum alloys: The role of surface morphology," *Int. J. Fatigue*, vol. 70, pp. 451–462, 2015.
- [10] J. Lemaître and J. L. Chaboche, *Mechanics of solid materials*. Cambridge, UK: Cambridge University Press, 1990.
- [11] M. Benedetti, V. Fontanari, M. Allahkarami, J. C. Hanan, and M. Bandini, "On the combination of the critical distance theory with a multiaxial fatigue criterion for predicting the fatigue strength of notched and plain shot-peened parts," *Int. J. Fatigue*, vol. 93, pp. 133–147, 2016.

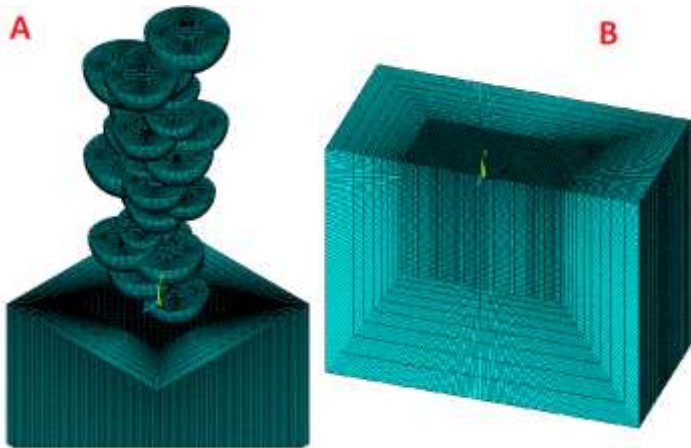


Figure 2
The FEM model.

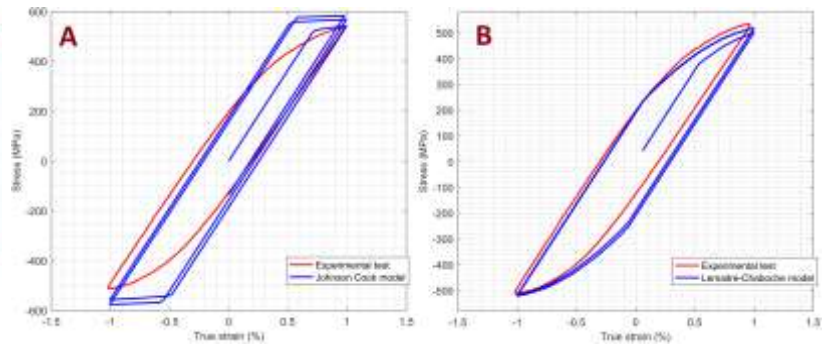


Figure 1
Comparison between the experimental stress-strain curves and the Johnson-Cook (A) and Lemaitre-Chaboche (B) models.

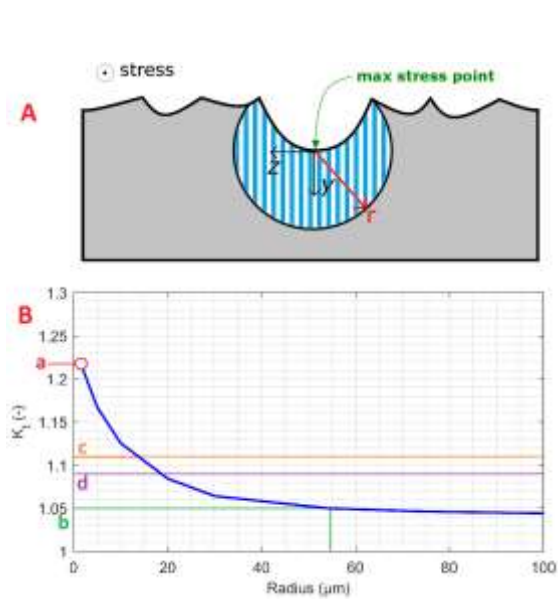


Figure 3
(A) Scheme of the simulation to compute K_t .
(B) K_t vs radius of the influence area.

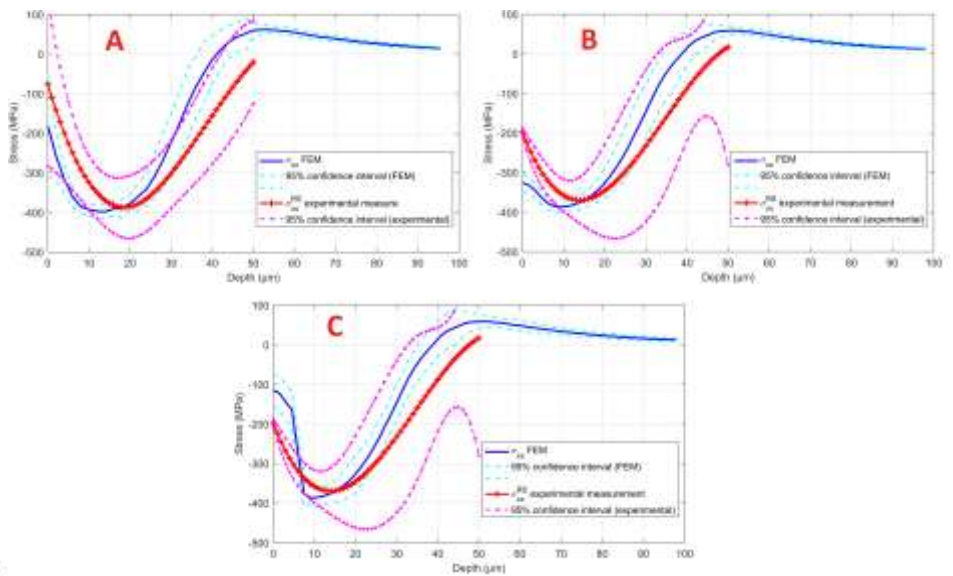


Figure 4
In-depth RS profile computed following the tree strategies.